

Magnetic properties of 4d impurities on the (001) surfaces of nickel and iron

B. Nonas, K. Wildberger, R. Zeller, and P. H. Dederichs

Institut für Festkörperforschung, Forschungszentrum Jülich GmbH, D-52425 Jülich, Germany

B. L. Gyorffy

H.H. Wills Physics Laboratory, University of Bristol, Bristol BS8 1TL, United Kingdom

(Received 25 July 1997)

We present *ab initio* calculations on the magnetic properties, in particular the surface enhancement, of single 4d transition-metal impurities on the (001) surfaces of the ferromagnets Fe and Ni. The calculations are based on local-density-functional theory and apply a KKR-Green's function method for defects on surfaces. We calculate the local moments of impurities in the adatom and in-surface positions and compare with the results obtained for bulk impurities. Contrary to the large local moments found for 4d impurities on the surfaces of the noble metals, our calculations predict only a moderate magnetic enhancement at the surfaces of the ferromagnets. [S0163-1829(98)05602-1]

I. INTRODUCTION

The magnetism of 4d elements recently received considerable attention. It is well known that all elemental 4d metals and 4d impurities in noble metal hosts are nonmagnetic, whereas 3d impurities show very large moments in these hosts. On the other hand, Riegel *et al.*¹ have shown that 4d impurities in the open lattices of alkali and alkali earth metals are strongly magnetic. *Ab initio* calculations² give indeed very large *d* moments compatible with Hund's rules for the atoms, e.g., $5\mu_B$ for a Mo impurity in K or Rb.

Due to the reduced coordination at surfaces, it is found that magnetic moments of monolayers and the surface moments of ferromagnets are strongly enhanced. The calculations of Blügel³ and others⁴ predict magnetic 4d monolayers; e.g., a Ru monolayer on Ag or Au(001) should have a local moment of $1.7\mu_B$, while for a Rh monolayer a moment of about $1.1\mu_B$ is estimated. Higher coordination at the surfaces attenuates the overlayer moments due to the increased hybridization as has been shown for Ru and Rh overlayers on Ag(111) where the moment decreases to 70% of the (001) value.⁵ Recent calculations⁶ for single transition-metal adatoms on the (001) surfaces of Cu and Ag yield even larger values for the local moments. For instance, for Mo and Tc adatoms on Ag(001) as well as for the isoelectronic 5d adatoms W and Re, moments of about $(3.5-4)\mu_B$ are predicted. Only slightly smaller moments are obtained on the (001) surfaces of Pd and Pt.⁷ In general these moments also survive if the adatoms are incorporated as substitutional impurities in the first monolayer of the surface.

In this paper we investigate the magnetic behavior of 4d impurities as adatoms on the (001) surfaces of the ferromagnets Fe and Ni. As such the present paper represents an extension of the previous work of the authors⁸ for 3d impurities on these surfaces. As it is well known from experimental and theoretical studies for impurities in the bulk of ferromagnets,⁹ the spin polarization of the host introduces two additional complications. First, the host polarization induces a local moment on the impurity sites, even if the impurities themselves are 'intrinsically' nonmagnetic. Sec-

ond, the impurity moments can couple either ferromagnetically or antiferromagnetically to the host moment, with the sign of the coupling changing in the middle of the series, from antiferromagnetic coupling for the early transition-metal impurities to ferromagnetic coupling for the late ones. The main emphasis of the present paper lies therefore on the surface enhancements of the 4d impurity moments and on the sign and strength of the coupling.

The outline of the paper is as follows. In the next section we shortly discuss the calculational method. In Sec. III we present the results of the calculations for 4d impurities on or in the surfaces of Fe and Ni(001) and compare with the corresponding results for bulk impurities as well as with results obtained for 3d and 4d adatoms on noble metal surfaces. Section IV concludes the paper.

II. CALCULATIONAL METHOD

Our calculations are based on density functional theory in the local-spin-density approximation and the Korringa-Kohn-Rostoker (KKR) Green's function method for defects on surfaces. In the KKR scheme the Green's function of the Kohn-Sham equation is separated by use of multiple-scattering theory into a single-scattering part of individual lattice sites and into a multiple-scattering part, containing the structural information of the considered system,

$$G(\mathbf{r}+\mathbf{R}_n, \mathbf{r}'+\mathbf{R}'_n, E) = \delta_{nn'} \sqrt{E} \sum_L R_L^n(\mathbf{r}_{<}, E) H_L^n(\mathbf{r}_{>}, E) + \sum_{LL'} R_L^n(\mathbf{r}, E) G_{LL'}^{nn'}(E) R_{L'}^{n'}(\mathbf{r}', E),$$

where L is the usual angular momentum index. \mathbf{R}_n denotes the atomic positions, \mathbf{r} refers to the position in the Wigner-Seitz (WS) cell and E is the energy. The first term describes the Green's function of a single potential $V^n(\mathbf{r})$ in free space, whereas the structural Green's function coefficients $G_{LL'}^{nn'}$ in

the second term take all multiple-scattering processes into account. The regular $R_L^n(\mathbf{r})$ and irregular $H_L^n(\mathbf{r})$ single-site scattering solutions are calculated by integration of the homogeneous radial Kohn-Sham equations and the structural Green's function is determined by an algebraic Dyson equation

$$G_{LL'}^{nn'}(E) = \overset{\circ}{G}_{LL'}^{nn'}(E) + \sum_{n''L''L'''} \overset{\circ}{G}_{LL''}^{nn''}(E) \Delta t_{L''L'''}^{n''}(E) G_{L''L'''}^{n''n'}(E)$$

with $\Delta t_{LL'}^n(E) = t_{LL'}^n(E) - \overset{\circ}{t}_{LL'}^n(E)$,

which relates the structural part of the Green's function $G_{LL'}^{nn'}$, of the considered system via the transition matrices $t_{LL'}^n(E)$ to the structural Green's function of a reference system $\overset{\circ}{G}_{LL'}^{nn'}(E)$. In the following calculations angular momenta up to $l_{\max}=3$ are included.

The reference system used for the following impurity calculations is either the undisturbed surface (in the case of adatoms on the surface or impurities in the first layer) or the ideal bulk (in the case of bulk defects). For bcc iron self-consistent calculations are carried out by considering in addition to the impurity potential also the potentials of the nearest and next-nearest neighbors as perturbed, whereas the calculations for the less open fcc nickel substrate include only perturbations of the nearest neighbors of the impurity. The scattering potentials are assumed to be spherically symmetric, but a multipole expansion of the charge density up to $l=6$ is used to take the intercell contributions of the potential into account. Lattice relaxations are neglected in our calculations so that the atoms remain fixed at ideal lattice sites. Following simple size arguments the $4d$ atoms at the surfaces considered here will presumably relax outwards, thus increasing the local moments. We think that neglecting this effect will qualitatively not influence the results presented in this paper focusing on the relative changes in local moments, but at present no definite answer to this question can be given. The exchange and correlation effects are included in the local-spin-density approximation, using the parameters by Vosko *et al.*¹⁰ Relativistic effects are described in the scalar relativistic approximation. For more details about the calculational method we refer to Refs. 6 and 11.

III. RESULTS AND DISCUSSION

In this section we present the results of our calculations for $4d$ impurities on the (001) surfaces of bcc Fe and fcc Ni. In particular we study the influence of the impurity position as well as the influence of the substrate on the local magnetic moments of the impurities. We consider impurity atoms in three different configurations: as adsorbate atoms at the hollow position in the first vacuum layer, as surface impurities at an ideal lattice site in the first surface layer, and as substitutional impurities in the bulk.

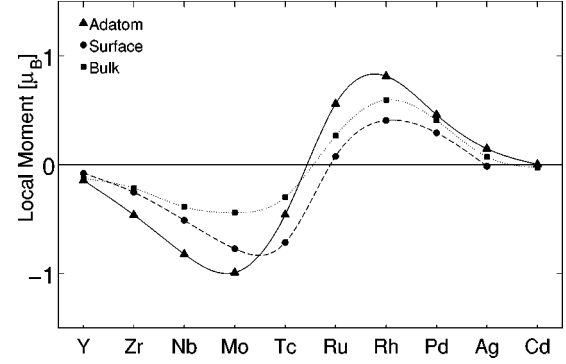


FIG. 1. Local moments of $4d$ impurities as adatoms on the Fe(001) surface (triangles), as impurities in the first surface layer (circles), and as impurities in the bulk (squares). (The connecting lines are a guide to the eye.)

A. Results for Fe(001)

Figure 1 shows the calculated local moments of $4d$ atoms as adsorbate and surface atoms on the Fe(001) surface and as impurities in bulk Fe. In all three cases we find an antiferromagnetic coupling for the early $4d$ impurities up to Tc and a ferromagnetic coupling for Ru, Rh, and Pd. As indicated by the lines the transition from antiferro- to ferromagnetic coupling is continuous, which is substantiated by calculations for noninteger nuclear charges. All adatom moments are enhanced compared to the moments of the bulk impurities, typically by a factor of about 2. However, when we compare these moments with the ones found for the $4d$ adatoms on the Cu or Ag(001) surfaces, being, e.g., for Mo or Tc as large as $(3-4)\mu_B$, we realize that the enhancement on Fe(001) is rather modest. The “intrinsic” moments of the impurities are to a large extent quenched by the strong hybridization of the extended $4d$ -wave functions with the also extended $3d$ -wave functions of the substrate, so that only relatively small “induced” moments are obtained.

But whereas the moments of the antiferromagnetically coupling surface impurities are enhanced, the ferromagnetic Ru, Rh, and Pd impurities in the surface layer have moments smaller than in the bulk, despite the fact that the coordination number is decreased. This anomaly can be explained by investigating the local density of states (LDOS) for both configurations. Figure 2 shows the LDOS of the majority and minority electrons for a Ru impurity in the surface position (dotted line) and in bulk Fe (solid line). For the surface position the LDOS of the minority electrons shows a peak slightly below the Fermi energy, which is absent in the bulk. This peak increases the number of minority electrons and, due to charge neutrality, decreases the population in the majority band, thus decreasing the local moment. The peak itself is connected with a surface state of the Fe(001) surface, which is characteristic for the bcc structure. The same effect also explains the increase of the (negative) moment of the Tc surface atom above the adatom value.

Figure 3 shows a comparison of the local moments of the $4d$ adatoms with the ones calculated for $3d$ adatoms on Fe(001).⁸ The open symbols refer to calculations for hypothetical noninteger nuclear charges, which have been performed to clarify the trend of the coupling. A characteristic feature of the $3d$ adatoms and surface atoms is the two-state

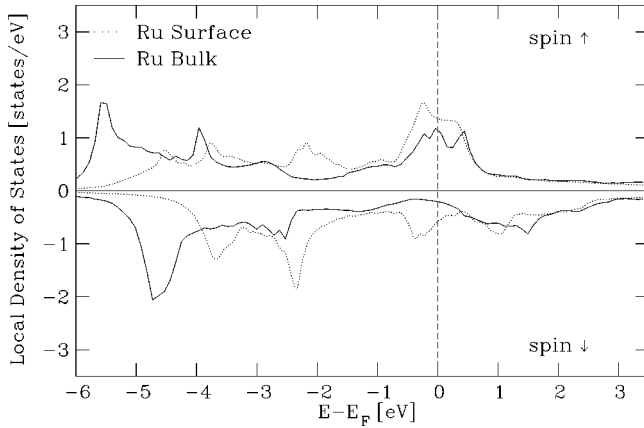


FIG. 2. Local density of states of a Ru impurity in the surface layer of Fe(001) (dotted line) and in bulk Fe (solid line). The surface state below the Fermi energy in the minority band decreases the local moment of the impurity on the surface site below the bulk value.

region in the middle of the series, leading to a first-order transition between the antiferro- and the ferromagnetic configuration. The third solution with a nearly vanishing moment corresponds to an energy maximum (or saddle point). For Mn the two solutions are nearly degenerate, with the adatom preferring the ferro- and the surface atom favoring the antiferromagnetic configuration.⁸ This clearly shows the “intrinsic” nature of the $3d$ moments versus the induced origin of the $4d$ ones.

The same behavior shows up if we compare the LDOS of two isoelectronic impurities of the $3d$ and $4d$ series. Figure 4 shows the spin-polarized LDOS of a Rh adatom and a Co adatom (isoelectronic to Rh) on Fe(001). Due to the much stronger hybridization of the $4d$ -wave functions with the host wave functions the average bandwidth of Rh is considerably broadened. This and the resulting smaller exchange integrals of the $4d$ elements decrease the tendency for magnetism and lead to smaller moments ($0.8\mu_B$ for Rh versus $1.8\mu_B$ for Co).

B. Results for Ni(001)

Figure 5 shows the calculated local moments of $4d$ impurities on the Ni(001) surface for the above considered configurations. As in Fig. 3 the open symbols refer to calculations for noninteger nuclear charges. One can see that the moments of the $4d$ impurities in the first Ni layer are slightly enhanced. Compared to this there is a substantial enhancement of the $4d$ adatom moments, in particular for Tc and Ru with moments of about $2\mu_B$. However, the transition from ferro- to antiferromagnetic coupling is continuous, in contrast to the behavior found for the $3d$ adatoms on Fe or Ni (Fig. 6). Nevertheless, we find for Tc further antiferromagnetic solutions with moments of $-1\mu_B$ and $-2\mu_B$ but with an energy higher than the ferromagnetic one. Interestingly the topology of the moment-versus-nuclear-charge curve is different from the one for $3d$ adatoms on Fe and Ni (Fig. 6).

At the end we compare the local magnetic moments of $4d$ adatoms on Fe and Ni(001) with the local moments of the same adatoms on Cu(001) and the corresponding results obtained for $3d$ adatoms on these substrates.⁷ For the case of

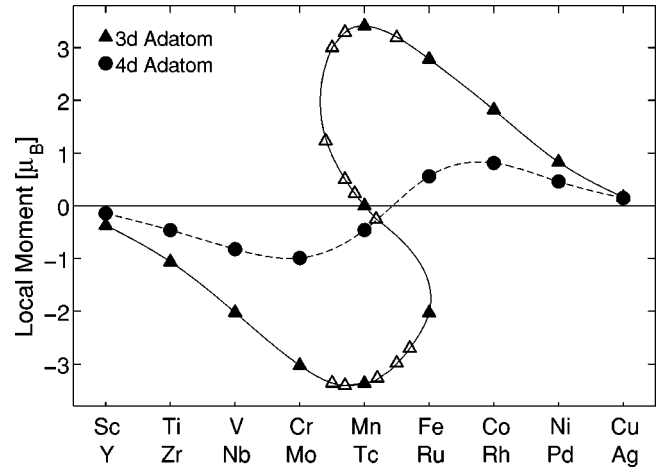


FIG. 3. Local moments of $4d$ and $3d$ impurities as adatoms on the Fe(001) surface. The open symbols refer to calculations for noninteger nuclear charge values.

the nonmagnetic Cu substrate the positive and negative moments are both plotted, since the corresponding states are degenerate. For the $3d$ adatoms on Ni(001) the hybridization with the substrate is sufficiently weak so that a broad two-magnetic-state region exists resembling very much the results for Cu. On the other hand, for the Fe substrate the hybridization is much stronger and the two-state region shrinks considerably. In fact, for the $3d$ impurities in bulk Fe a very sharp but continuous transition is obtained, leading to an anomalously small Mn moment of $0.8\mu_B$. Analogously to the behavior of $3d$ adatoms, the $4d$ adatoms show large and stable moments on the Cu substrate. On the other hand, on the Ni substrate the moments are considerably reduced and the transition becomes continuous, except for the Tc adatom where also antiferromagnetic solutions exist. On the Fe substrate the increased hybridization reduces the $4d$ moments further so that essentially only the induced part of the moments remains. The induced nature of the moments can clearly be seen at the beginning and end of the series. Since these adatoms are nonmagnetic on the Cu substrate, the resulting induced moments should scale with the strength of the hybridization and the size of the exchange splitting of the substrate. Therefore these elements show larger moments on

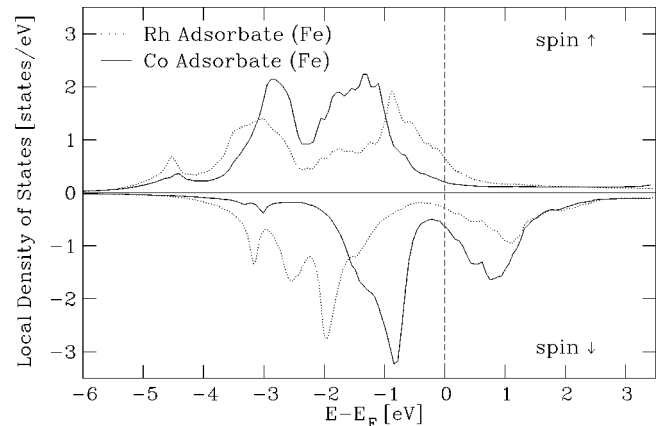


FIG. 4. Spin-polarized density of states of a Rh adatom and its isoelectronic $3d$ partner Co on the Fe(001) surface.

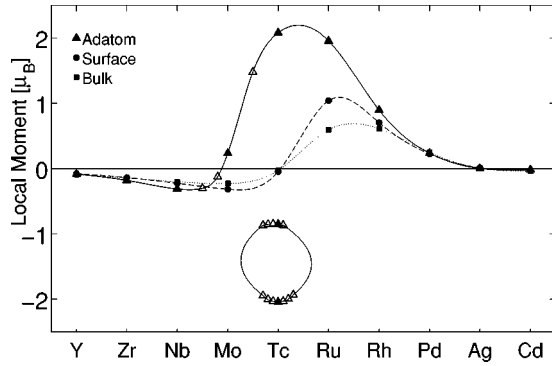


FIG. 5. Local moments of 4d impurities on the Ni(001) surface (triangles), in the first surface layer (circles), and in the bulk (squares).

the Fe than on the Ni(001) surface. This reversed order of the magnitude of the moments is found at the beginning and end of both the 4d and 3d series.

IV. SUMMARY

We presented KKR-Green's function calculations for the electronic structure and local moments of 4d impurities on the (001) surfaces of bcc Fe and fcc Ni. Three different configurations are considered: adatoms in the first vacuum layer, impurities in the surface layer, and impurities in the bulk. We find for both substrates a surface enhancement of the local moments, which is largest for the adatom configuration. Exceptions are the ferromagnetically coupling impurities Ru, Rh, and Pd on Fe(001) which have a smaller moment in the surface layer than in the bulk. This anomaly is caused by the minority surface state of Fe(001). The coupling of the impurity moments to the substrate moments changes from antiferromagnetic at the beginning of the series to ferromagnetic at the end. The broad two-magnetic-state region in the 3d series leads to a first-order transition, whereas the transition in the 4d series is continuous. In general, the 4d moments are relatively small and to a large extent induced by the substrate magnetization. This is very different from the large local moments found for the same impurities on noble metal surfaces. With moments of about $2\mu_B$, only Tc and Ru adatoms on Ni(001) represent an intermediate case which resembles the behavior found for the noble metals.

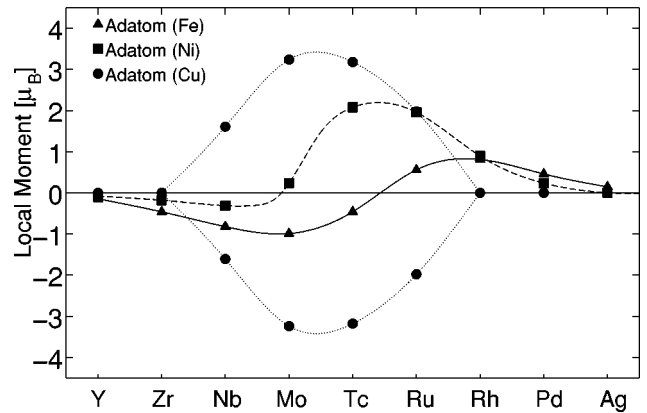
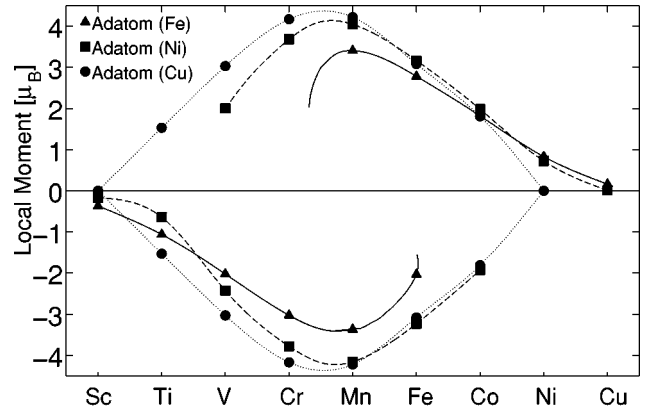


FIG. 6. Local moments of 3d atoms (above) and 4d atoms (below) as calculated for the (001) surfaces of iron, nickel, and copper.

ACKNOWLEDGMENTS

This work profited from collaborations within the TMR-Network "Interface Magnetism" of the European Union. We acknowledge financial support within the Schwerpunktprogramm "Relativistic effects" of the Deutsche Forschungsgemeinschaft.

¹D. Riegel, K.D. Gross, and M. Luszik-Bhadra, Phys. Rev. Lett. **59**, 1244 (1987).

²N. Papanikolaou, N. Stefanou, R. Zeller, and P.H. Dederichs, Phys. Rev. B **46**, 10 858 (1992).

³S. Blügel, Phys. Rev. Lett. **68**, 851 (1992).

⁴M.J. Zhu, D.M. Bylander, and L. Kleinmann, Phys. Rev. B **43**, 4007 (1991).

⁵J. Redinger, S. Blügel, and R. Podloucky, Phys. Rev. B **51**, 13 852 (1995).

⁶P. Lang, V.S. Stepanyuk, K. Wildberger, R. Zeller, and P.H. Dederichs, Solid State Commun. **92**, 755 (1994).

⁷V.S. Stepanyuk, W. Hergert, K. Wildberger, R. Zeller, and P.H.

Dederichs, Phys. Rev. B **53**, 2121 (1996).

⁸B. Nonas, K. Wildberger, R. Zeller, and P.H. Dederichs, J. Magn. Magn. Mater. **165**, 137 (1997).

⁹B. Drittler, N. Stefanou, S. Blügel, R. Zeller, and P.H. Dederichs, Phys. Rev. B **40**, 8203 (1989).

¹⁰S. H. Vosko, L. Wilk, and M. Nusair, J. Chem. Phys. **58**, 1200 (1980).

¹¹R. Zeller, P. Lang, B. Drittler, and P.H. Dederichs, in *Application of Multiple Scattering Theory to Materials Science*, edited by W. H. Butler *et al.*, MRS Symposia Proceedings No. 253 (Materials Research Society, Pittsburgh, 1992), p. 357.